

A shell model for superfluids in rough-walled nanopores

Wang Yang¹ and Ian Affleck¹

¹*Department of Physics and Astronomy and Stewart Blusson Quantum Matter Institute, University of British Columbia, Vancouver, B.C., Canada, V6T 1Z1*

Recent experiments on the flow of helium-4 fluid through nanopores with tunable pore radius provide a platform for studying the quasi-one-dimensional (quasi-1D) superfluid behaviors. In the extreme 1D limit, the helium atoms are localized by disordered small variations in the substrate potential provided by the pore walls. In the limit of wide pore radius, a solid layer of helium-4 is expected to coat the pore walls smoothing out the substrate potential, and superfluidity is observed in the central region. Building on earlier quantum Monte Carlo results, we propose a scenario for this crossover using a shell model of coupled Luttinger liquids. We find that a small radius pore will always localize the helium atoms, but above a critical radius, a single 1D channel flows through the pore and can be described by Luttinger liquid theory.

I. INTRODUCTION

Superfluidity in bosonic helium-4 can be characterized by flow through narrow pores or constrictions with zero viscosity^{1,2}. The walls of such pores are never perfectly smooth, but will always be characterized by some combination of disorder and periodic modulation associated with the solid material through which they traverse. Thus, as helium atoms flow through the pore, they will necessarily experience a spatially dependent potential. Although the detail of this potential is material dependent, its origin lies in the dipole-dipole or Van der Waals interaction between helium atoms and the atoms in the surrounding substrate. A ubiquitous feature of such potentials is the presence of a deep potential minima near the surface of the pore. This is responsible for the phenomena of wetting³ and drives the escape of superfluid helium from an open container. In a confined nanopore geometry, the potential has an approximately cylindrical symmetry, and the wetting layer will instead form a shell, localized near the pore walls. For any excess helium atoms inside this shell, its presence helps to smooth out the localizing effects of disorder or commensuration with the wall, and allows for a superfluid component to remain to flow through the center of the pore.

On the other hand, a host of recent experiments aim to study the quasi-one-dimensional (quasi-1D) properties of helium-4 confined inside regular nanometer sized constrictions. Examples of the restricted geometries include solid helium cells in contact with superfluid helium^{4,5}, networks of edge dislocations⁶, and nanopores in mesoporous materials⁷⁻²¹. An alternative approach has been undertaken to study helium-4 mass flow in a single cylindrical nanopore, carved with an electron beam through a thin Si₃N₄ membrane¹⁶. A major motivation for these experiments is to study the crossover of a quantum fluid to the 1D regime. A fluid of interacting bosons at low temperatures (T) confined to move along an infinite line is predicted to be a “Luttinger liquid”²², a sort of quasi-superfluid with power law decay at $T = 0$ of the superfluid correlation function $\langle \psi^\dagger(x)\psi(y) \rangle \propto |x - y|^{-K/2}$ where $\psi(x)$ is the boson annihilation operator. Such a

liquid is characterized at low energies by its Luttinger parameter K , which is a measure of the tendency towards algebraically decaying superfluid or solid order.

On the theory side, grand canonical quantum Monte Carlo (QMC) simulations have been performed for helium confined inside smooth nanopores^{23,24}, where realistic interactions between helium atoms and the walls of a translationally invariant Si₃N₄ pore were included at a chemical potential corresponding to the bulk three-dimensional (3D) saturated vapor pressure. It was found that a pore of radius $R = 2.9\text{\AA}$ will support a single quasi-1D column of atoms which can be described at low temperature by Luttinger liquid theory with a large value of $K = 6.0 \pm 0.2$ ²⁴. QMC studies on smooth cylindrical pores with larger radii observed the formation of multiple circular layers inside the pore^{24,25} and a significantly slower decay of the superfluid correlation function near the pore center. In Fig. 1, QMC configuration snapshots illustrating this behavior are shown for a nanopore with length $L = 10\text{nm}$ at $T = 0.75K$ for $R = 3-15\text{\AA}$.

In real Si₃N₄ pores, it is expected that there would be a large confining potential with both periodic and random components due to the glassy structure of the substrate and irregularities in the pore produced by the high energy electron beam. Even a small external potential is predicted to localize a 1D Luttinger liquid for sufficiently large K , with the critical values of K being $1/2$ for a periodic potential commensurate with the helium density and $2/3$ for a random potential²⁶. Thus we should expect that experiments on small-radius narrow pores, if possible, would not detect any fluid flow at least for small pressure gradients. On the other hand, as explained previously, bulk 3D superfluid behavior is expected when the pore radius reaches the micron range, regardless of the presence of a sizable substrate potential.

In this work, based on the results of the QMC simulations in Ref. 23,24, we develop an analytical theory and propose a shell model of coupled Luttinger liquids to analyze the effects of disordered wall potentials, where the Luttinger liquid channels correspond to the shells of concentrated helium atoms as shown in Fig. 1. Each channel is expected to have a large Luttinger parameter

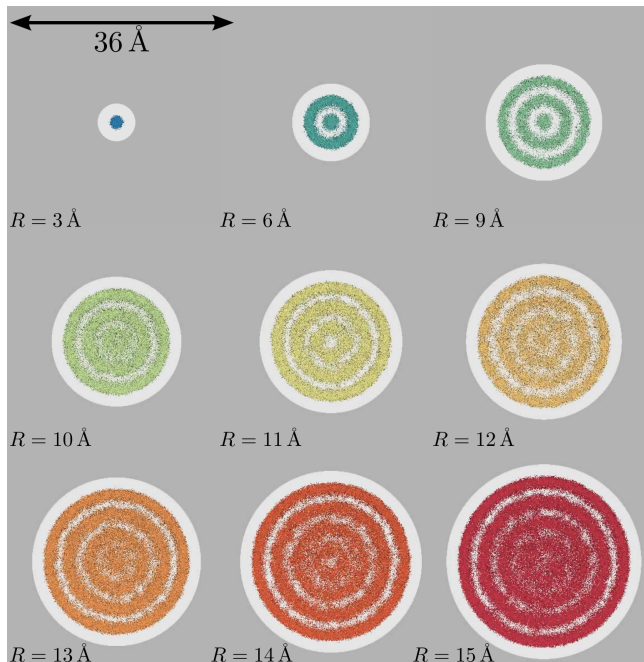


FIG. 1: Quantum Monte Carlo configurations (particle world lines) projected onto a plane at $T = 0.75K$ for helium-4 atoms confined inside silicon nitride nanopores with radii between $R = 3\text{--}15\text{\AA}$ and length $L = 10nm$. The azimuthal symmetry in conjunction with a strong confining potential leads to a mass density that oscillates as a function of radius due to the spontaneous formation of concentric cylindrical shells. For full simulation details see Ref. 24.

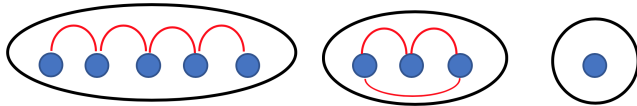


FIG. 2: Collective groups of channels bound by the relevant inter-shell tunneling operators at low energies. The solid blue circles represent different Luttinger liquid channels in the absence of inter-shell interactions, inter-shell tunnelings and disorders. The red line represents the relevant tunneling term between the two channels which the line connects. The solid black circles represent the group of channels that are bound by the relevant inter-shell tunneling operators in the RG sense. In this case, $P = 9$ and $Q = 3$.

K due to intra-shell interactions. The couplings between different channels arise from inter-shell hoppings and the residual inter-shell interactions. We find that the repulsive inter-shell interactions always lower the Luttinger parameters, at least for small interaction strengths. If the Luttinger parameters are rendered small enough, the inter-shell hoppings become relevant at low energies in the sense of renormalization group (RG), and are able to pin the superfluid phases of the corresponding shells among which the hoppings take place. As a result, the P Luttinger liquid channels are regrouped into Q ($\leq P$) bound entities, such that at low energies, the channels

within each entity share a same superfluid phase. An illustration of such regrouping is shown in Fig. 2. In particular, the Luttinger parameters of the groups of bound channels will be significantly lowered, making them more immune to disorder effects.

Based on this analysis, we propose a scenario of the crossover behavior from narrow to wide nanopores: the helium atoms are localized by the random substrate potential for small radius pores, whereas there exists a critical radius value, above which a single (grouped) channel Luttinger liquid emerges in the central region of the nanopore. This scenario indicates that the large Luttinger parameter in 1D helium-4 does not necessarily destroy the hope of observing the 1D to 3D crossover in experiments and may actually make it easier due to the resulting increase in the critical pore radius. It would be desirable to compare the predictions here with QMC simulations as well as real experiments.

Finally, we also note the whole analysis does not necessarily rely on the decomposition of channels based on cylindrical shells. Other ways of choosing the channels, for example, angular momentum decomposition, work equally well, which is discussed in Sec. IV A.

The rest of the paper is organized as follows. In Sec. II, the model Hamiltonian is introduced and the bosonization is performed. In Sec. III, the effects of inter-shell interactions on the scaling dimensions of the inter-shell tunnelings are analyzed. In Sec. IV, the low energy theory for the Hamiltonian including the inter-shell interactions and inter-shell tunnelings is derived. Based on the results in the previous sections, Sec. V discusses the effects of disordered substrate potential. Finally in Sec. VI, we briefly summarize the main results of the paper.

II. THE MODEL HAMILTONIAN

It is a familiar idea that the single particle quantum wave-functions in an infinitely long small radius pore correspond to a set of sub-bands with different transverse wave-vectors. However, that is not the approach we are using here. As indicated in Fig. 1, for pore radii of 4\AA or greater, several concentric cylindrical shells of helium atoms form inside the nanopore. This is a consequence of the Aziz potential²⁷ describing the interaction between helium atoms and also the potential used to model the interaction with the smooth wall of the pore. The density of helium atoms is suppressed at radii between the shells, motivating a starting point in which tunneling (i.e., hopping) of atoms between shells is ignored.

Then, for suitably long pores, each shell may be considered as an independent 1D system, giving a P -channel Luttinger liquid for a pore with P shells. Each of these shells will have a different linear density of atoms and different effective 1D inter-atomic interactions. At least three effects need to be included if this model is to be used to describe the physics of quantum fluids in real nanopores: inter-shell interactions, inter-shell tunneling,

and the substrate potential which we might expect to be larger on the outer shells near the pore wall than on the inner shells. This model corresponds to a multi-leg ladder, with each leg corresponding to a shell.

We consider the Hamiltonian of P channels of Luttinger liquids, as

$$H = H_0 + H_{\text{int}} + H_T, \quad (1)$$

in which: H_0 is the sum of intra-channel terms

$$H_0 = \sum_{i=1}^P \left[\int dx \psi_i^\dagger \left(-\frac{\hbar^2}{2m} \frac{d^2}{dx^2} - \mu_i \right) \psi_i + \frac{1}{2} \int dx dy \rho_i(x) \hat{U}_{ii}(x-y) \rho_i(y) \right], \quad (2)$$

where ψ_i^\dagger , μ_i and $\rho_i(x) = \psi_i^\dagger(x) \psi_i(x)$ are the boson creation operator, the chemical potential and the density operator, respectively, in the i 'th channel; H_{int} includes the inter-shell density-density interactions as

$$H_{\text{int}} = \sum_{1 \leq i < j \leq P} \int dx dy \rho_i(x) \hat{U}_{ij}(x-y) \rho_j(y); \quad (3)$$

and H_T is the inter-shell tunneling term

$$H_T = \sum_{1 \leq i < j \leq P} \int dx dy [t_{ij}(x-y) \psi_i^\dagger(x) \psi_j(y) + \text{h.c.}], \quad (4)$$

where ‘‘h.c.’’ is ‘‘hermitian conjugate’’ for short. Later we will also include the substrate/disorder potential H_S given by

$$H_S = \sum_{i=1}^P \int dx V_i(x) \rho_i(x), \quad (5)$$

in which $V_i(x)$ represents the substrate/disorder potential acting in the i 'th channel.

The above Hamiltonians can be expressed in bosonized forms. We introduce the bosonization fields $\theta_i(x)$, $\phi_i(x)$, such that $\psi_i(x)$ and $\rho_i(x)$ can be expressed in terms of $\theta_i(x)$, $\phi_i(x)$ using the following bosonization formulas²²,

$$\begin{aligned} \psi_i(x) &= \sqrt{\rho_{0i} + \frac{1}{\pi} \frac{d\theta_i(x)}{dx}} e^{-i\phi_i(x)}, \\ \rho_i(x) &= \rho_{0i} + \frac{1}{\pi} \frac{d\theta_i(x)}{dx} + [\text{const.} \times e^{2\pi i \rho_{0i} x - 2i\theta_i(x)} + \text{h.c.}], \end{aligned} \quad (6)$$

in which $\theta_i(x)$, $\phi_i(x)$ satisfy the commutation relations

$$[\theta_i(x), \phi_j(y)] = \frac{\pi}{2} \delta_{ij} \text{sgn}(x-y), \quad (7)$$

and ρ_{0i} is the average density in the i 'th channel.

After bosonization, H_0 acquires the form

$$H_0 = \frac{1}{2\pi} \int dx \sum_{i=1}^P \left\{ v_{Ji} \left[\frac{d\phi_i(x)}{dx} \right]^2 + v_{Ni} \left[\frac{d\theta_i(x)}{dx} \right]^2 \right\}, \quad (8)$$

in which the Luttinger parameter K_i and the velocity v_{si} are related to v_{Ni} and v_{Ji} by

$$K_i = \sqrt{\frac{v_{Ni}}{v_{Ji}}}, \quad v_{si} = \sqrt{v_{Ni} v_{Ji}}. \quad (9)$$

For later convenience, we write H_0 in a matrix form

$$H_0 = \frac{1}{2\pi} \int dx \nabla \theta^T V_N \nabla \theta + \frac{1}{2\pi} \nabla \phi^T V_J \nabla \phi, \quad (10)$$

in which θ and ϕ are both P -components column vectors defined as

$$\theta = (\theta_1, \dots, \theta_P)^T, \quad \phi = (\phi_1, \dots, \phi_P)^T, \quad (11)$$

and V_J , V_N are diagonal matrices whose matrix elements are given by

$$(V_N)_{ij} = v_{Ni} \delta_{ij}, \quad (V_J)_{ij} = v_{Ji} \delta_{ij}. \quad (12)$$

The inter-shell interaction term H_{int} acquires the bosonized form

$$H_{\text{int}} = \frac{1}{\pi^2} \sum_{i < j=1}^P \int dx \hat{U}_{ij} \frac{d\theta_i}{dx} \frac{d\theta_j}{dx}, \quad (13)$$

in which we have only kept the local terms, and the oscillating terms in the density operators drop off the expression under the assumption that different channels have different densities ρ_{0i} . H_{int} can also be written in a matrix form

$$H_{\text{int}} = \frac{1}{\pi^2} \int dx \nabla \theta^T U \nabla \theta, \quad (14)$$

in which the matrix elements of U are given by

$$U_{ij} = (1 - \delta_{ij}) \hat{U}_{ij}. \quad (15)$$

Notice that unlike \hat{U} in Eq. (3), the diagonal matrix elements of U are all zero. Here we note that the two-leg version of this model was studied in Ref. 28 in the special case where the two legs are equivalent, having equal densities and velocity parameters. In our case, the occurrence of different densities actually simplifies the analysis since the coupling of oscillating density operators $\cos\{2\pi(\rho_{0i} - \rho_{0j})x - 2[\theta_i(x) - \theta_j(x)]\}$ can be dropped from the low energy theory due to the oscillating phase.

The inter-shell tunneling terms in Eq. (4) acquires the bosonized form

$$H_T = \sum_{1 \leq i < j \leq P} t_{ij} \int dx \cos(\phi_i - \phi_j). \quad (16)$$

Finally, the disorder term can be bosonized as

$$H_S = \sum_{j=1}^P \int dx V_j(x) \cos[2\pi \rho_{0j} x - 2\theta_j(x)]. \quad (17)$$

III. THE INTER-SHELL INTERACTIONS

In this section, we consider the effects of inter-shell interactions. As will be discussed in Sec. III A, the Hamiltonian remains quadratic by including the inter-shell interactions and can be diagonalized by performing a canonical transformation. Then in Sec. III B, we determine the scaling dimensions of the inter-shell tunneling terms.

A. Canonical transformation

Including the inter-shell interactions, the Hamiltonian $H_1 = H_0 + H_{\text{int}}$ becomes

$$H_1 = \frac{1}{2\pi} \int dx [\nabla\theta^T (V_N + \frac{1}{\pi}U)\nabla\theta + \nabla\phi^T V_J \nabla\phi]. \quad (18)$$

Define θ' and ϕ' as

$$\phi' = V_J^{1/2}\phi, \quad \theta' = V_J^{-1/2}\theta, \quad (19)$$

then H_1 can be written as

$$H_1 = \frac{1}{2\pi} \int dx [\nabla\theta'^T V'_N \nabla\theta' + \nabla\phi'^T \nabla\phi'], \quad (20)$$

in which

$$V'_N = V_J^{1/2}(V_N + \frac{1}{\pi}U)V_J^{1/2}, \quad (21)$$

and the matrix kernel of the ϕ' term becomes the $P \times P$ identity matrix.

Let O be an orthogonal matrix that diagonalizes V'_N i.e.,

$$V'_N = O\Lambda_\theta O^T, \quad (22)$$

where Λ_θ is a diagonal matrix, and define

$$\phi'' = O^T \phi', \quad \theta'' = O^T \theta', \quad (23)$$

then we obtain

$$H_1 = \frac{1}{2\pi} \int dx [\nabla\theta''^T \Lambda_\theta \nabla\theta'' + \nabla\phi''^T \nabla\phi'']. \quad (24)$$

The Luttinger parameter K_j'' in the j 'th channel is given by the j 'th eigenvalue of V'_N , i.e.,

$$K_j'' = \sqrt{(\Lambda_\theta)_{jj}}. \quad (25)$$

Here we note that the Luttinger parameter K_j'' is not dimensionless. This is because after the transformation Eq. (19), the new coordinates ϕ', θ' acquire dimensions, unlike the original canonical coordinates ϕ, θ which are dimensionless. Alternatively, one can introduce an arbitrary velocity v_0 into Eq. (19), such that the transformations become $v_0^{1/2}\phi' = V_J^{1/2}\phi$ and $v_0^{-1/2}\theta' = V_J^{-1/2}\theta$. Then K_j'' becomes dimensionless which is dependent on the scale v_0 . However, we will keep using Eq. (19) in this paper for simplification of notations, since this does not affect any physical observable.

B. Scaling dimensions of inter-shell tunnelings

The scaling dimension of the field $e^{i\lambda\phi_j''}$ is²⁶

$$[e^{i\lambda\phi_j''}] = \frac{1}{4}\lambda^2 K_j'', \quad (26)$$

where [...] denotes the scaling dimension of the operator inside the bracket. Thus, to get the scaling dimensions of the tunneling terms $\cos(\phi_i - \phi_j)$'s, we need to rewrite $\phi_i - \phi_j$ in terms of ϕ_j'' .

Denote \hat{e}_i to be the P -dimensional unit column vector along the i 'th direction, i.e.,

$$\hat{e}_i = (0, \dots, 0, 1, 0, \dots, 0)^T, \quad (27)$$

in which 1 appears at the i 'th position. Let

$$x_{ij} = \hat{e}_i - \hat{e}_j, \quad (28)$$

then $\phi_i - \phi_j = \phi_j^T x_{ij}$. Using Eqs. (19,23), we obtain $\phi_j^T x_{ij} = \phi_j''^T y_{ij}$, in which

$$y_{ij} = O^T V_J^{-1/2} x_{ij}. \quad (29)$$

Notice that the scaling dimension of $\cos(\phi_j''^T y)$ is

$$d_{ij} = \frac{1}{4} \sum_{l=1}^P [(y_{ij})_l]^2 K_l'' = \frac{1}{4} y_{ij}^T \Lambda_\theta^{1/2} y_{ij}, \quad (30)$$

where $(y_{ij})_l$ is the l 'th component of the column vector y_{ij} , and K_l'' is given by Eq. (25). Using Eqs. (22,29), we obtain

$$d_{ij}(U) = \frac{1}{4} x_{ij}^T V_J^{-1/2} \sqrt{(V_s)^2 + \frac{1}{\pi} V_J^{1/2} U V_J^{1/2}} V_J^{-1/2} x_{ij}, \quad (31)$$

in which $V_s = \sqrt{V_N V_J}$.

Since V_s^2 in general does not commute with $\frac{1}{\pi} V_J^{1/2} U V_J^{1/2}$, the square root $\sqrt{V_s^2 + \frac{1}{\pi} V_J^{1/2} U V_J^{1/2}}$ cannot be easily carried out. We will consider this square root in the limit of a small U , and only keep the results up to first order in the matrix elements U_{ij} . To proceed, the following lemma is needed and a proof is included in Appendix A.

Lemma. Let A and B both be real symmetric matrices. Suppose A is also positive definite. Then

$$\left[\frac{d}{d\lambda} \sqrt{A + \lambda B} \right]_{\lambda=0} = \int_0^\infty dt e^{-t\sqrt{A}} B e^{-t\sqrt{A}}. \quad (32)$$

Now we apply Eq. (32) to our case. By taking $A = V_s^2$ and $B = \frac{1}{\pi} V_J^{1/2} U V_J^{1/2}$, we obtain

$$\begin{aligned} & \sqrt{V_s^2 + \frac{1}{\pi} V_J^{1/2} U V_J^{1/2}} - V_s \\ &= \int_0^\infty dt e^{-tV_s} \left(\frac{1}{\pi} V_J^{1/2} U V_J^{1/2} \right) e^{-tV_s} + O(U^2). \end{aligned} \quad (33)$$

Thus, to linear order in U , $\Delta d_{ij} = d_{ij}(U) - d_{ij}(U=0)$ can be expressed as

$$\begin{aligned} \Delta d_{ij} &= \\ \frac{1}{4} x_{ij}^T V_J^{-1/2} & \left[\int_0^\infty dt e^{-tV_s} \left(\frac{1}{\pi} V_J^{1/2} U V_J^{1/2} \right) e^{-tV_s} \right] V_J^{-1/2} x_{ij}. \end{aligned} \quad (34)$$

Notice that both V_s and V_J are diagonal matrices, hence they commute. Using the expressions for x_{ij} , we obtain

$$\begin{aligned} \Delta d_{ij} &= \frac{1}{4\pi} \int_0^\infty dt x_{ij}^T e^{-tV_s} U e^{-tV_s} x_{ij} \\ &= -\frac{U_{ij}}{2\pi} \int_0^\infty dt e^{-t(v_{si}+v_{sj})} \\ &= -\frac{U_{ij}}{2\pi(v_{si}+v_{sj})}, \end{aligned} \quad (35)$$

in which $v_{sj} = (V_s)_{jj}$.

In summary, the scaling dimension of $\cos(\phi_i - \phi_j)$ is given by

$$d_{ij}(U) = \frac{1}{4}(K_i + K_j) - \frac{U_{ij}}{2\pi(v_{si} + v_{sj})} + O(U^2). \quad (36)$$

Therefore, the repulsive inter-shell interactions always lower the scaling dimensions of the inter-shell tunneling terms, at least for small U . In particular, this indicates that the inter-shell tunnelings are rendered more relevant at low energies in the RG sense.

IV. LOW ENERGY THEORY WITH INTER-SHELL TUNNELINGS

A. The gapless modes of center of mass motions

Now we are prepared to discuss the effects of inter-shell tunnelings. In general, some of the tunneling operators are relevant, while some are irrelevant. We will build up the low energy theory for $H = H_0 + H_{\text{int}} + H_T$ by integrating over the modes which are rendered massive by the relevant tunneling terms. As a consequence, the number of Luttinger liquid channels at low energies is reduced.

Since $K_i \sim 6$ ($1 \leq i \leq P$),²⁴ the value of d_{ij} in Eq. (36) is around 3 in the absence of inter-shell interactions. According to Eq. (36), repulsive interactions always lower the scaling dimensions d_{ij} . If d_{ij} becomes smaller than 2, then the corresponding tunneling $\cos(\phi_i - \phi_j)$ is relevant and flows to the strong coupling limit at low energies. Graphically, as shown in Fig. 2, we connect the two channels by a solid line if the tunneling term between them is a relevant operator. In this way, the P channels can be partitioned into Q ($\leq P$) groups. Within each group, any two channels are connected by a path formed by the solid lines, whereas for two channels in two different groups, there is no path connecting them.

Let's consider the i 'th group containing P_i channels, where $\sum_{i=1}^Q P_i = P$. An example is shown in Fig. 2, in which $P_1 = 5$, $P_2 = 3$, $P_3 = 1$, and $P = 9$, $Q = 3$. Let $\{i_1, \dots, i_{P_i}\}$ be the numberings of the channels in the i 'th group. Then in the strong coupling limit, the tunneling potential becomes

$$\sum_{1 \leq k < l \leq P_i} T_{i_k i_l} \cos(\phi_{i_k} - \phi_{i_l}), \quad (37)$$

in which we have denoted $T_{i_k i_l} = b^{2-d_{i_k i_l}} t_{i_k i_l}$ as the RG flowed coupling at low energies when the cutoff is reduced by a factor of b . We note that not all $T_{i_k i_l}$'s are nonzero. If $d_{i_k i_l}$ is larger than 2, then the corresponding $T_{i_k i_l}$ vanishes. However, by assumption, any two channels within $\{i_1, \dots, i_{P_i}\}$ can be connected by a path of nonzero $T_{i_k i_l}$'s. We also note that $T_{i_k i_l}$ can be either positive or negative depending on the sign of the bare tunneling term $t_{i_k i_l}$. The strategy is to perform a mean field (i.e., classical) analysis to the RG flowed potential in Eq. (37). In the strong coupling limit, the ground state of the system is determined by minimizing the potential in Eq. (37). The simplest situation is when all $T_{i_k i_l}$'s are negative. Then the minimum solution is given by $\phi_{i_k} \equiv \phi_i^{(0)}$ where $1 \leq k \leq P_i$ and $\phi_i^{(0)}$ is some arbitrary real number.

For general $T_{i_k i_l}$'s, we assume that $\phi_{i_k} = \phi_{i_k}^{(0)}$ ($1 \leq k \leq P_i$) is a minimum solution. Apparently, translating all ϕ_{i_l} 's by the same amount does not cost any energy, since the cosine potential only depends on the difference $\phi_{i_k} - \phi_{i_l}$. Therefore, the shifted coordinates

$$\phi_{i_k} = \phi_{i_k}^{(0)} + \lambda, \quad \lambda \in \mathbb{R} \quad (38)$$

also minimizes the potential. Hence, the shift of an overall phase is a gapless mode, and it corresponds to the center of mass motion of all the P_i channels within the i 'th group.

Supposing we have found a minimum solution of the tunneling potential in the strong coupling limit for each group of channels, next we expand Eq. (37) around the minimum solutions. Let $\delta\phi_{i_l}$ defined as

$$\delta\phi_{i_l} = \phi_{i_l} - \phi_{i_l}^{(0)} \quad (39)$$

be the coordinate parametrizing the deviation from the minimum solution. Then the tunneling potential can be expanded in a Taylor expansion of $\delta\phi_{i_l}$. The linear terms vanish since $\{\phi_{i_l}^{(0)}\}_{1 \leq l \leq P_i}$ constitutes a saddle point. Keeping only the quadratic terms, the tunneling potential becomes

$$\frac{1}{2\pi} \delta\phi^T M \delta\phi, \quad (40)$$

in which M is a $P \times P$ symmetric and semi-positive-definite matrix.

Notice that M contains Q zero eigenvalues, corresponding to translating all the ϕ_j 's within the same group

of channels by a same amount of displacement. More explicitly, the vector w_k defined as

$$w_k = (0, \dots, 1, 0, \dots, 1, \dots, 0)^T \quad (41)$$

is a null vector of M (i.e., $Mw_k = 0$), in which the “1”’s appear at the k_1, \dots, k_{P_k} positions. The massive modes in Eq. (40) can be integrated out. Hence, at low energies, it is enough to keep the Q gapless modes. Our next step is to write down the low energy theory for these Q Luttinger liquid modes, which will be discussed in Secs. IV B, IV C. We will first diagonalize the Hamiltonian for the $q = 0$ sector. Then a nonzero wavevector can be included by a $k \cdot p$ perturbation on the Q gapless modes in the $q = 0$ case.

Here we make a comment on the choice of decomposing the channels. Although we have based our discussions on a shell model of coupled Luttinger liquids, it can be readily observed that the whole discussion does not rely how the channels are defined. For example, one can define the channels according to the angular momentum decomposition of the wavefunctions in a cylindrical geometry. In that case, the regrouping of channels discussed in this section due to inter-channel tunnelings equally applies. The subsequent discussions in Secs. IV B, IV C, V essentially only rely on a collection of regrouped channels, not dependent on how these regrouped entities arise. Hence, our analysis is based on a flexible scheme which captures the overall features and is not sensitive to the microscopic details.

B. The zero wavevector Hamiltonian

We first consider the $q = 0$ case. The Hamiltonian is given by

$$H(q=0) = \frac{1}{2\pi} \nabla \theta^T(q=0) (V_N + \frac{1}{\pi} U) \nabla \theta(q=0) + \frac{1}{2\pi} \delta \phi^T(q=0) M \delta \phi(q=0), \quad (42)$$

in which $\nabla \theta_j(q=0)$ is the canonical conjugate partner of $\delta \phi_j(q=0)$. In what follows, we will drop $q = 0$ for simplification of notations. To diagonalize H , we first diagonalize $V_N + \frac{1}{\pi} U$, then rescale it to an identity matrix, and finally diagonalize M .

The real symmetric matrix $V_N + \frac{1}{\pi} U$ can be diagonalized by an orthogonal matrix O_1 as

$$V_N + \frac{1}{\pi} U = O_1 A_\theta O_1^T, \quad (43)$$

in which A_θ is a diagonal matrix. Define the transformed coordinates $\theta^{(1)}$ and $\delta \phi^{(1)}$ as $\theta^{(1)} = O_1^T \theta$, $\delta \phi^{(1)} = O_1^T \delta \phi$. Then the θ -part in Hamiltonian is diagonalized with matrix kernel A_θ . Next rescale $\theta^{(1)}$, $\delta \phi^{(1)}$ according to $\theta^{(2)} = A_\theta^{1/2} \theta^{(1)}$, $\delta \phi^{(2)} = A_\theta^{-1/2} \delta \phi^{(1)}$, then $H = \frac{1}{2\pi} \nabla \theta^{(2),T} \nabla \theta^{(2)} + \frac{1}{2\pi} \delta \phi^{(2),T} \tilde{M} \delta \phi^{(2)}$, where

$$\tilde{M} = A_\theta^{1/2} O_1^T M O_1 A_\theta^{1/2}. \quad (44)$$

Since \tilde{M} is symmetric, it can be diagonalized by an orthogonal matrix O_2 , as

$$\tilde{M} = O_2 \Lambda_\phi O_2^T, \quad (45)$$

where Λ_ϕ is diagonal. Define $\tilde{\theta} = O_2^T \theta^{(2)}$, $\delta \tilde{\phi} = O_2^T \delta \phi^{(2)}$, we obtain

$$H = \frac{1}{2\pi} \nabla \tilde{\theta}^T \nabla \tilde{\theta} + \frac{1}{2\pi} \delta \tilde{\phi}^T \Lambda_\phi \delta \tilde{\phi}. \quad (46)$$

In summary, under the transformations

$$\begin{aligned} \tilde{\theta} &= O_2^T A_\theta^{1/2} O_1^T \theta, \\ \delta \tilde{\phi} &= O_2^T A_\theta^{-1/2} O_1^T \delta \phi, \end{aligned} \quad (47)$$

the Hamiltonian at $q = 0$ is transformed into Eq. (46). In what follows, for Λ_ϕ , we will take the convention of arranging the zero eigenvalues in the upper-left block, and put the remaining massive eigenvalues to the later positions on the diagonal line, i.e.,

$$\Lambda_\phi = \begin{pmatrix} 0 & & & & & \\ & \dots & & & & \\ & & 0 & & & \\ & & & m_1 & & \\ & & & & \dots & \\ & & & & & m_{P-Q} \end{pmatrix}, \quad (48)$$

in which there are Q zeros among the diagonal elements. We are going to relate the Q canonical pairs of the collective gapless modes $\{\theta_k, \delta \tilde{\phi}_k\}_{1 \leq k \leq Q}$ with the coordinates $\{\theta_j, \delta \phi_j\}_{1 \leq j \leq P}$, which will be used in deriving the $q \neq 0$ Hamiltonian.

Before proceeding on, let's try to gain a better understanding of the structure of O_2 . If Φ_k is a null vector of M , then $\tilde{\Phi}_k$ given by

$$\tilde{\Phi}_k = A_\theta^{-1/2} O_1^T \Phi_k \quad (49)$$

must be a null vector of \tilde{M} (as defined in Eq. (44)). We emphasize that this is not true for the eigenvectors of other eigenvalues, i.e., if Φ is an eigenvector of M with a nonzero eigenvalue, then $\Lambda_\theta^{-1/2} O_1^T \Phi$ may not necessarily be an eigenvector of \tilde{M} . By assuming Φ_k to be the “center of mass” motion of the k 'th group of channels as discussed in Eq. (38), it is clear that $\Phi_k \propto w_k$ where w_k is defined in Eq. (41). To determine the normalization of Φ_k , notice that $\tilde{\Phi}_k$ is a column of the orthogonal matrix O_2 , hence $\tilde{\Phi}_k$ is normalized to 1, i.e., $\tilde{\Phi}_k^T \tilde{\Phi}_k = 1$. This fixes the normalization of Φ_k to be

$$\Phi_k = \frac{1}{\sqrt{\sum_{l=1}^{P_k} [(A_\theta)_{k_l k_l}]^{-1}}} (\hat{e}_{k_1} + \dots \hat{e}_{k_{P_k}}), \quad (50)$$

in which e_j and A_θ are defined in Eq. (27) and Eq. (43), respectively, and $(A_\theta)_{k_l k_l}$ represents the matrix element of A_θ at the (k_l, k_l) position. Since \tilde{M} is diagonalized by

O_2 , we see that the k 'th column ($1 \leq k \leq Q$) of O_2 is $\tilde{\Phi}_k$, i.e.,

$$(O_2)_k^{cl} = \tilde{\Phi}_k \quad (51)$$

in which $(C)_k^{cl}$ denotes the column vector formed by the k 'th column of the matrix C . More explicitly,

$$O_2 = (\tilde{\Phi}_1, \dots, \tilde{\Phi}_k, \tilde{\Phi}'_{k+1}, \dots, \tilde{\Phi}'_P), \quad (52)$$

in which $\tilde{\Phi}'_j$ ($k+1 \leq j \leq P$) are the eigenvectors of the massive eigenvalues in Eq. (48).

Next, we express $\tilde{\theta}_k$ ($1 \leq k \leq Q$) – which is the gapless mode of the k 'th component of the column vector $\tilde{\theta}$ – in terms of θ_i 's ($1 \leq i \leq P$). According to Eq. (47), $\tilde{\theta}_k$ is equal to $[(O_2)_k^{cl}]^T A_\theta^{1/2} O_1^T \theta$. Using Eqs. (49,51), it is straightforward to obtain

$$\tilde{\theta}_k = \Phi_k^T \theta. \quad (53)$$

By virtue of Eq. (50), we conclude that for the ‘‘center of mass’’ motion of the k 'th group of channels $\{j_1, \dots, j_{P_k}\}$, the gapless mode is given by $\tilde{\theta}_k \propto \theta_{k_1} + \dots + \theta_{k_{P_k}}$. Here we make a comment on $(A_\theta)_{k_l k_l}$'s which appear in the normalization factor of Φ_k . According to Eq. (43), $(A_\theta)_{k_l k_l}$ is equal to $v_{N_{k_l}}$ up to lowest order in U . Since the diagonal elements of U vanish, the first order corrections of the eigenvalues of A_θ are zero. Hence, the next order term in $(A_\theta)_{k_l k_l}$ is in the order of U^2 , i.e.,

$$(A_\theta)_{k_l k_l} = v_{N_{k_l}} + O(U^2). \quad (54)$$

We also examine $\delta\tilde{\phi}$ and derive the component of $\delta\phi_i$ on $\delta\tilde{\phi}_k$ ($1 \leq k \leq Q$). Notice that $\delta\phi = O_1 A_\theta^{1/2} O_2 \delta\tilde{\phi}$. Thus the component of $\delta\phi$ on $\delta\tilde{\phi}_k$ is given by the k 'th column of $O_1 A_\theta^{1/2} O_2$. On the other hand, $(O_1 A_\theta^{1/2} O_2)_k^{cl} = (O_1 A_\theta^{1/2})(O_2)_k^{cl} = \Phi_k$, where Eqs. (49,51) are used. This shows that the component of $\delta\phi$ on $\delta\tilde{\phi}_k$ is given by Φ_k . Taken into account the normalization, we obtain

$$\delta\phi = \sum_{k=1}^Q \frac{1}{\sqrt{\sum_{l=1}^{P_k} [(A_\theta)_{k_l k_l}]^{-1}}} (\hat{e}_{k_1} + \dots + \hat{e}_{k_{P_k}}) \delta\tilde{\phi}_k + \text{massive modes}, \quad (55)$$

in which the notation ‘‘massive modes’’ in Eq. (55) denote the contributions from the massive eigenvectors $\delta\tilde{\phi}_k$ ($Q+1 \leq k \leq P$).

In summary, the transformations between $\{\tilde{\theta}, \delta\tilde{\phi}\}$ and $\{\theta, \delta\phi\}$ are given by Eqs. (53,55), and can be arranged into the following matrix forms

$$\begin{aligned} \tilde{\theta}^L &= \begin{pmatrix} \Phi_1^T \\ \dots \\ \Phi_k^T \end{pmatrix} \theta, \\ \delta\phi &= (\Phi_1, \dots, \Phi_k) \delta\tilde{\phi}^L + \text{massive modes}, \end{aligned} \quad (56)$$

in which $\tilde{\theta}^L$ and $\delta\tilde{\phi}^L$ are both Q -component column vectors defined as

$$\begin{aligned} \tilde{\theta}^L &= (\tilde{\theta}_1, \dots, \tilde{\theta}_Q)^T \\ \delta\tilde{\phi}^L &= (\delta\tilde{\phi}_1^L, \dots, \delta\tilde{\phi}_Q^L)^T, \end{aligned} \quad (57)$$

where $\tilde{\theta}_k^L, \delta\tilde{\phi}_k^L$ ($1 \leq k \leq Q$) are used to denote the gapless Luttinger liquid modes within $\tilde{\theta}_j, \delta\tilde{\phi}_j$ ($1 \leq j \leq P$). The components of $\delta\phi$ on $\delta\tilde{\phi}_l$ ($Q+1 \leq l \leq P$) are abbreviated in the notation ‘‘massive modes’’ and not explicitly shown.

Finally we note that besides the detailed derivations of the transformations in Eq. (56) given within this section, there are understandings of Eq. (56) based on considerations on general grounds. An understanding of Eq. (56) from the point of view of the Noether theorem is discussed in Appendix B, which in particular, does not rely on the Gaussian fluctuation approximation made in Eq. (40). In addition, the transformation from $\delta\phi$ to $\delta\tilde{\phi}$ can be inferred from that from θ to $\tilde{\theta}$ as discussed in Appendix C, since the two transformations together constitute a canonical transformation.

C. The nonzero wavevector Hamiltonian

Now we are able to write down the low energy theory for the Q gapless modes by including nonzero wavevectors, which can be achieved using a $k \cdot p$ perturbation theory. Comparing the Hamiltonians between the $q = 0$ and $q \neq 0$ cases, we see that there is one additional term for a nonzero q which involves the derivatives of $\delta\phi$, i.e.,

$$\Delta H(q) = \frac{1}{2\pi} \nabla \delta\phi^T(q) V_J \nabla \delta\phi(-q), \quad (58)$$

in which $\nabla \delta\phi = \nabla \phi$ is used and V_J is defined in Eq. (12). Notice that in the $k \cdot p$ treatment, we should replace ∇ in Eq. (56) by $\pm iq$, but we choose to keep the gradient symbol for simplicity.

By integrating out the massive modes, it is enough to keep the gapless modes $\delta\tilde{\phi}_k^L$ ($1 \leq k \leq Q$) in Eq. (58). Using Eq. (56), we obtain

$$\Delta H(q) = \frac{1}{2\pi} \nabla \delta\tilde{\phi}^{L,T}(q) \tilde{V}_J \nabla \delta\tilde{\phi}^L(-q), \quad (59)$$

in which

$$\tilde{V}_J = \begin{pmatrix} \Phi_1^T \\ \dots \\ \Phi_k^T \end{pmatrix} V_J (\Phi_1, \dots, \Phi_k). \quad (60)$$

Since V_J is diagonal, and different Φ_k 's do not have any common channel, it is clear that \tilde{V}_J is diagonal, i.e.,

$$\Phi_m^T V_J \Phi_n = (\tilde{V}_J)_{mm} \delta_{mn}, \quad 1 \leq m, n \leq Q. \quad (61)$$

The normalization factor can be straightforwardly calculated as

$$(\tilde{V}_J)_{kk} = \frac{\sum_{l=1}^{P_k} v_{J_{k_l}}}{\sum_{l=1}^{P_k} (A_\theta)_{k_l k_l}^{-1}}, \quad (62)$$

in which A_θ is defined in Eq. (43). Keeping only the $O(1)$ terms, we have

$$(\tilde{V}_J)_{kk} = \frac{\sum_{l=1}^{P_k} v_{Jk_l}}{\sum_{l=1}^{P_k} v_{Nk_l}^{-1}} + O(U^2). \quad (63)$$

In summary, the low energy theory for the Q gapless modes is

$$\tilde{H} = \frac{1}{2\pi} \sum_{k=1}^Q \int dx [\nabla \tilde{\theta}_k^L \nabla \tilde{\theta}_k^L + \tilde{v}_{Jk} \nabla \delta \tilde{\phi}_k^{L,T} \nabla \delta \tilde{\phi}_k^L], \quad (64)$$

in which the velocity and Luttinger parameter for the k 'th mode are

$$\tilde{v}_{Jk} = (\tilde{V}_J)_{kk}, \quad \tilde{K}_k = \frac{1}{\sqrt{\tilde{v}_{Jk}}}. \quad (65)$$

V. SUBSTRATE POTENTIAL

To understand the fate of the Q remaining gapless boson fields in Eq. (64) which are not pinned by inter-shell tunnelings, we must finally consider the effect of the substrate potential.

The bosonized form of the substrate potential is given in Eq. (17). If the substrate potential has a Fourier component at wave-vector $2\pi\rho_{0j}$, then the operator $\cos[2\theta_j(x)]$ will appear in the effective Hamiltonian and will be relevant if it has dimension $d_{Sj} < 2$. Alternatively, if the substrate potential has a random component at this wavevector, H_S will be relevant if²⁹ $d_{Sj} < 3/2$. However, to study the RG behaviour of H_S we must take into account the effects of the inter-shell tunnelings. These lead to competing phases since H_S attempts to pin the θ_j variables whereas H_T attempts to pin the ϕ_j variables. When a field is pinned, its dual field fluctuates strongly making the corresponding interaction irrelevant. Here we assume that the substrate potential is sufficiently weak compared to the inter-shell tunneling, such that Eq. (17) can be treated as a perturbation on Eq. (65). This assumption should be true at least for the channels in the central region of the nanopore when the radius of the pore is large.

Rewriting $\cos(2\theta_j)$ in the $\tilde{\theta}$ -basis always involves some of the $\tilde{\theta}_k$ variables with $k > Q$ (corresponding to massive modes) which makes H_T irrelevant. Thus inter-shell tunneling can stabilize the system against disorder. However, we must consider higher order processes which can be relevant. For example, the following term which involves the k 'th gapless collective mode ($1 \leq k \leq Q$) in Eq. (64) is allowed via a P_k 'th order perturbation,

$$H_S^{(i)} = \int dx V(x) \cos[2\pi\rho_{0,(k)}x - 2 \sum_{l=1}^{P_k} \theta_{k_l}], \quad (66)$$

in which $\rho_{0,(k)} = \sum_{l=1}^{P_k} \rho_{0k_l}$ is the total linear density in the k 'th group of channels. Taking into account the fact

that $V(x)$ may have a Fourier mode at $2\pi\rho_{0,(k)}$ and a random component, the relevance of $H_S^{(k)}$ is determined by the scaling dimension $d_{S,(k)}$ of $\cos[2 \sum_{l=1}^{P_k} \theta_{k_l}]$.

Using Eq. (56), $\cos[2 \sum_{l=1}^{P_k} \theta_{k_l}]$ can be rewritten as

$$\cos[2 \sum_{l=1}^{P_k} \theta_{k_l}] = \cos(2\mu_k \tilde{\theta}_k), \quad (67)$$

in which μ_k is given by $\mu_k = \sqrt{\sum_{l=1}^{P_k} [(A_\theta)_{k_l k_l}]^{-1}}$. Therefore, the scaling dimension $d_{S,(k)}$ can be determined as $d_{S,k} = \mu_k / \tilde{K}_k$. According to Eq. (65), we obtain

$$d_{S,k} = \sqrt{\left(\sum_{l=1}^{P_k} v_{Jj_l} \right) \left(\sum_{l=1}^{P_k} [(A_\theta)_{k_l k_l}]^{-1} \right)}. \quad (68)$$

To understand Eq. (68), let's consider the special case of identical P channels of Luttinger liquids without inter-shell interactions, i.e.,

$$v_{Ji} \equiv v_J, \quad v_{Ni} \equiv v_N, \quad (69)$$

where $1 \leq i \leq P$. Then it is clear that up to $O(U^0)$, we have

$$d_{S,k} = \sqrt{P_k^2 \frac{v_J}{v_N}} = \frac{P_k}{K}, \quad (70)$$

in which $K = \sqrt{\frac{v_J}{v_N}} \sim 6$ is the Luttinger parameter of a single channel in the initial model of P coupled Luttinger liquid channels. Thus we see that the larger P_k is, the more robust the k 'th gapless mode in Eq. (64) becomes with respect to disorder effects.

Finally, let's consider an example for illustration, which might be relevant to real situations with a large pore radius. For simplification, suppose initially there are P approximately identical channels satisfying Eq. (69). Assume that the inner $P-1$ channels are bound by inter-shell tunnelings and the outer P 'th channel is left decoupled. In this case, we have $Q = 2$. Then according to Eq. (70), the scaling dimensions of the disorder potentials are given by

$$d_{S,1} \sim \frac{P-1}{K}, \quad d_{S,2} \sim \frac{1}{K}, \quad (71)$$

where $K \sim 6$. Clearly, the outermost P 'th shell is localized by the disorder which coats the pore wall. For the inner $P-1$ shells, they are localized by the disordered substrate potential when P is small. However, $d_{S,1}$ can be made arbitrarily large by increasing P , hence the effect of disorder potential on the inner entity of the $P-1$ shells will be made irrelevant for sufficiently large P . As a result, we should be able to observe a Luttinger liquid flowing through the nanopore.

We note that the above analysis provides an understanding to the physical arguments about the 1D to 3D

crossover behavior as discussed in Sec. I. The P 'th shell is pinned by the wall potential and shields the inner fluids from the substrate such that superfluidity (here quasi-long ranged superfluidity) is maintained in the central regions. For more complicated situations, we expect that as long as the pore radius is large enough, there exists a group of shells which are bound together by inter-shell tunnelings, making them robust to disorder effects. Therefore, a Luttinger liquid channel always exists in the system for nanopores with a large enough radius.

VI. CONCLUSION

In conclusion, based on earlier QMC observations, we propose a shell model of coupled Luttinger liquids to describe the helium-4 mass flow through rough-walled nanopores. Using this shell model, the effects of substrate potential and increasing pore radius are studied. For small pore radius, all helium-4 atoms are localized by the substrate potential. However, at a critical radius, a single component gapless Luttinger liquid emerges as the first step in the crossover to 3D behavior. This result is related to the standard picture for larger pores where a layer of bosons near the pore wall smooth out the substrate potential and allow a tube of atoms to flow through the center with zero viscosity. It suggests that there may be a range of pore radii over which single component Luttinger liquid behavior could be observed. Surprisingly, this does not require such a small radius that there is only one shell. Rather the minimum required pore radius corresponds to multiple shells in order for the effects of the substrate potential to be screened. Numerical test of the proposed scenario is worth further studies.

Acknowledgments We thank A. Del Maestro and S. Sahoo for helpful discussions. WY and IA acknowledge support from NSERC Discovery Grant 04033-2016.

Appendix A: Proof of Eq. (32)

In this appendix, following Ref. 30, we give a quick proof of Eq. (32). Let $A(\lambda) = A + \lambda B$. Let D be defined as

$$D = \left[\frac{d}{d\lambda} \sqrt{A + \lambda B} \right]_{\lambda=0}, \quad (\text{A1})$$

i.e., $D = \left[\frac{d}{d\lambda} \sqrt{A(\lambda)} \right]_{\lambda=0}$. Differentiating $[\sqrt{A(\lambda)}]^2 = A(\lambda)$, we have

$$D\sqrt{A} + \sqrt{A}D = \left[\frac{d}{d\lambda} A(\lambda) \right]_{\lambda=0} = B, \quad (\text{A2})$$

which has a unique solution for D . We show that the integral expression for D in Eq. (32) satisfies Eq. (A2).

In fact,

$$\begin{aligned} & D\sqrt{A} + \sqrt{A}D \\ &= \int_0^\infty dt [e^{-t\sqrt{A}} B e^{-t\sqrt{A}} \sqrt{A} + \sqrt{A} e^{-t\sqrt{A}} B e^{-t\sqrt{A}}] \\ &= \int_0^\infty dt \left(-\frac{d}{dt} \right) (e^{-t\sqrt{A}} B e^{-t\sqrt{A}}) \\ &= B, \end{aligned} \quad (\text{A3})$$

completing the proof of Eq. (32).

Appendix B: Noether theorem and the collective gapless modes

For simplification, we consider the special case of $Q = 1$, i.e., there is only one gapless mode, which corresponds to the center of mass motion of all the P channels. The general case of an arbitrary Q can be discussed in a similar manner by considering the channels of each collective gapless mode separately.

To apply the Noether theorem, we consider the original Hamiltonian in Eq. (1) in its bosonized form. The system has a continuous symmetry defined as

$$\phi_i \rightarrow \phi_i + \lambda, \quad (\text{B1})$$

where $1 \leq i \leq P$, and $\lambda \in \mathbb{R}$. The corresponding Noether current is

$$j^\mu = \sum_i \frac{\partial \mathcal{L}}{\partial (\partial_\mu \phi_i)}, \quad (\text{B2})$$

in which $\mu = 0$ and 1 corresponding to the time and spatial coordinates, respectively, and the Lagrangian \mathcal{L} density is given by

$$\begin{aligned} \mathcal{L} &= \frac{1}{\pi} \sum_i \partial_t \phi_i \partial_x \theta_i - \frac{1}{2\pi} \sum_i [v_{Ji} (\partial_x \phi_i)^2 + v_{Ni} (\partial_x \theta_i)^2] \\ &\quad - \frac{1}{\pi^2} \sum_{i < j} \hat{U}_{ij} \partial_x \theta_i \partial_x \theta_j - \sum_{i,j} t_{ij} \cos(\phi_i - \phi_j). \end{aligned} \quad (\text{B3})$$

This gives

$$\begin{aligned} j^0 &= \frac{1}{\pi} \sum_i \partial_x \theta_i, \\ j^1 &= -\frac{1}{\pi} \sum_i v_{Ji} \partial_x \phi_i. \end{aligned} \quad (\text{B4})$$

The local conservation law

$$\partial_\mu j^\mu = 0 \quad (\text{B5})$$

then implies

$$\partial_t \sum_i \partial_x \theta_i = \sum_i v_{Ji} \partial_x^2 \phi_i. \quad (\text{B6})$$

Multiplying both sides of Eq. (B6) by Φ_1^T , where, according to Eq. (50), Φ_1 is defined as

$$\Phi_1 = \frac{1}{\sqrt{\sum_{l=1}^P [(A_\theta)_{ll}]^{-1}}} (1, \dots, 1)^T, \quad (\text{B7})$$

Eq. (B6) can then be alternatively written as

$$\partial_t \partial_x \tilde{\theta}_1 = \Phi^T V_J \partial_x^2 \phi, \quad (\text{B8})$$

in which V_J is the matrix defined in Eq. (12), and $\tilde{\theta}_1$ represents the collective coordinate of the center of mass motion defined in Eq. (56). Notice that the designation of the coordinate as $\tilde{\theta}_1$ is consistent with the convention taken in Eq. (48), where the numbering of the gapless modes are in front of the massive modes. Using Eq. (56), $\partial_x^2 \phi$ can be expressed in terms of $\partial_x^2 \delta \tilde{\phi}_i$'s. Then Eq. (B8) becomes

$$\partial_t \partial_x \tilde{\theta}_1 = \Phi^T V_J \Phi \cdot \partial_x^2 \delta \tilde{\phi}_1 + \partial_x^2 (\text{massive modes}). \quad (\text{B9})$$

According to Eq. (60), Eq. (B9) is simply

$$\partial_t \partial_x \tilde{\theta}_1 = (\tilde{v}_J)_1 \partial_x^2 \delta \tilde{\phi}_1 + \partial_x^2 (\text{massive modes}). \quad (\text{B10})$$

At low energies, the massive modes can be removed from Eq. (B9). Thus Eq. (B10) coincides exactly with the equation of motion for $\partial_x \tilde{\theta}_1$ which can be readily derived from the Hamiltonian in Eq. (64). This provides an understanding of Eq. (64) in terms of conservation law and Noether theorem.

Appendix C: Canonical transformation from $\{\theta, \delta\phi\}$ to $\{\tilde{\theta}, \delta\tilde{\phi}\}$

Consider the following linear transformations

$$\tilde{\theta} = U_\theta \theta, \quad \delta \tilde{\phi} = U_\phi \delta \phi, \quad (\text{C1})$$

in which both U_α ($\alpha = \theta, \phi$) are $P \times P$ matrices. Assuming $\{\tilde{\theta}, \delta \tilde{\phi}\}$ to satisfy the same commutation relations as $\{\theta, \delta \phi\}$, i.e., Eq. (7), it is straightforward to obtain

$$U_\theta U_\phi^T = I_P, \quad (\text{C2})$$

where I_P represents the $P \times P$ identity matrix. Therefore, we obtain $\delta \tilde{\phi} = U_\theta^{-1, T} \delta \phi$, or alternatively,

$$\delta \phi = U_\theta^T \delta \tilde{\phi}. \quad (\text{C3})$$

This is exactly Eq. (56).

In summary, according to Appendices B, we see that the expression of $\tilde{\theta}$ is fixed by Noether theorem, since its spatial derivative $\partial_x \tilde{\theta}$ simply corresponds to the Noether charge. Then the transformation for $\delta \tilde{\phi}$ is determined from the property of the canonical transformation as discussed in this appendix. However, we emphasize that the usefulness of Eq. (C1) in diagonalizing the Hamiltonian is based on the Gaussian fluctuation approximation made in Eq. (40).

-
- ¹ J. Wilks, *Liquid and Solid Helium* (Clarendon, Oxford, 1967).
- ² A. J. Leggett, *Quantum Liquids* (Oxford University Press, Oxford, U.K., 2006).
- ³ de Gennes, *Rev. Mod. Phys.* **57**, 827 (1985).
- ⁴ Ye. Vekhov and R. B. Hallock, *Phys. Rev. Lett.* **109**, 045303 (2012).
- ⁵ M. W. Ray and R. B. Hallock, *Phys. Rev. Lett.* **100**, 235301 (2008).
- ⁶ M. Boninsegni, A. B. Kuklov, L. Pollet, N. V. Prokof'ev, B. V. Svistunov, and M. Troyer, *Phys. Rev. Lett.* **99**, 035301 (2007).
- ⁷ P. E. Sokol, M. R. Gibbs, W. G. Stirling, R. T. Azuah, and M. A. Adams, *Nature* **379**, 616 (1996).
- ⁸ S. Inagaki, A. Koiwai, N. Suzuki, Y. Fukushima, and K. Kuroda, *Bull. Chem. Soc. Jpn.* **69**, 1449 (1996).
- ⁹ R. M. Dimeo, P. E. Sokol, D. W. Brown, C. R. Anderson, W. G. Stirling, M. A. Adams, S. H. Lee, C. Rutiser, and S. Komarneni, *Phys. Rev. Lett.* **79**, 5274 (1997).
- ¹⁰ R. M. Dimeo, P. E. Sokol, C. R. Anderson, W. G. Stirling, K. H. Andersen, and M. A. Adams, *Phys. Rev. Lett.* **81**, 5860 (1998).
- ¹¹ O. Plantevin, B. Fåk, H. R. Glyde, N. Mulders, J. Bossy, G. Coddens, and H. Schøber, *Phys. Rev. B* **63**, 224508 (2001).
- ¹² C. R. Anderson, K. H. Andersen, W. G. Stirling, P. E. Sokol, and R. M. Dimeo, *Phys. Rev. B* **65**, 174509 (2002).
- ¹³ O. Plantevin, H. R. Glyde, B. Fåk, J. Bossy, F. Albergamo, N. Mulders, and H. Schber, *Phys. Rev. B* **65**, 224505 (2002).
- ¹⁴ R. Toda, M. Hieda, T. Matsushita, N. Wada, J. Taniguchi, H. Ikegami, S. Inagaki, and Y. Fukushima, *Phys. Rev. Lett.* **99**, 255301 (2007).
- ¹⁵ J. Taniguchi, R. Fujii, and M. Suzuki, *Phys. Rev. B* **84**, 134511 (2011).
- ¹⁶ M. Savard, G. Dauphinais, and G. Gervais, *Phys. Rev. Lett.* **107**, 254501 (2011).
- ¹⁷ T. R. Prisk, N. C. Das, S. O. Diallo, G. Ehlers, A. A. Podlesnyak, N. Wada, S. Inagaki, and P. E. Sokol, *Phys. Rev. B* **88**, 014521 (2013).
- ¹⁸ J. Taniguchi, K. Demura, and M. Suzuki, *Phys. Rev. B* **88**, 014502 (2013).
- ¹⁹ Ohba, *Sci. Rep.*, **6**, 28992 (2016).
- ²⁰ M. S. Bryan, T. R. Prisk, T. E. Sherline, S. O. Diallo, and P. E. Sokol, *Phys. Rev. B* **95**, 144509 (2017).
- ²¹ J. Bossy, J. Ollivier, and H. R. Glyde, *Phys. Rev. B* **99**, 165425 (2019).
- ²² D. Haldane, *Phys. Rev. Lett.* **57**, 1849 (1981).
- ²³ A. D. Maestro and I. Affleck, *Phys. Rev. B* **82**, 060515R (2010).

- ²⁴ A. Del Maestro, M. Bonninsegni and I. Affleck, Phys. Rev. Lett. **106**, 105303 (2011).
- ²⁵ B. Kulchytsky, G. Gervais and A. Del Maestro, Phys. Rev. B, **88**, 064512 (2013).
- ²⁶ T. Giamarchi, *Quantum Physics in One Dimension* (Clarendon Press, Oxford, 2004).
- ²⁷ R. A. Aziz, V. P. S. Nain, J. S. Carley, W. L. Taylor, and G. T. McConville, J. Chem. Phys. **70**, 4330 (1979).
- ²⁸ E. Orignac and T. Giamarchi, Phys. Rev. B **57**, 11713 (1998).
- ²⁹ T. Giamarchi and H. J. Schulz, Phys. Rev. B **37**, 325 (1988).
- ³⁰ J.R. Magnus, H. Neudecker, *Matrix Differential Calculus*, Wiley, New York, 1988.